Single Extracellular Vesicle Protein Analysis Using Immuno-Droplet Digital Polymerase Chain Reaction Amplification

Jina Ko, Yongcheng Wang, Jonathan C. T. Carlson, Angela Marquard, Jeremy Gungabeesoon, Alain Charest, David Weitz, Mikael J. Pittet, and Ralph Weissleder*

There is a need for novel analytical techniques to study the composition of single extracellular vesicles (EV). Such techniques are required to improve the understanding of heterogeneous EV populations, to allow identification of unique subpopulations, and to enable earlier and more sensitive disease detection. Because of the small size of EV and their low protein content, ultra-high sensitivity technologies are required. Here, an immuno-droplet digital polymerase chain reaction (iddPCR) amplification method is described that allows multiplexed single EV protein profiling. Antibody–DNA conjugates are used to label EV, followed by stochastic microfluidic incorporation of single EV into droplets. In situ PCR with fluorescent reporter probes converts and amplifies the barcode signal for subsequent read-out by droplet imaging. In these proof-of-principle studies, it is shown that multiplex protein analysis is possible in single EV, opening the door for future analyses.

1. Introduction

Single cell analysis continues to have a major impact on our understanding of cell subtypes, biology, and medicine.[1,2] The same is likely true for analyses of single exosomes or extracellular vesicles (EV) in general. It has become apparent that EV populations can be even more heterogeneous than the parental cells from which they are derived.[3,4] This is likely due to selective shedding of proteins and nucleic acid cargo, the much smaller size and payload capacity of EV, and stochastic cellular effects. In order to use EV more efficiently as biomarkers of disease, we need a better understanding of their composition and heterogeneity.

A number of single EV analytical methods have been proposed. These include analysis by microscopic imaging of immobilized vesicles (SEA),[5,6] modified flow cytometry,[5,7–10] and digital detection using ELISA[11] or nucleic acid-based amplification.[28] In spite of this progress, it remains challenging to detect rare proteins in single EV, given the inherent signal/background limitations of direct fluorescence imaging and relatively modest enzyme mediated signal amplification in ELISA.

Here we describe a new method for ultrasensitive detection of proteins in single EV that exploits antibody-based immuno-droplet digital polymerase chain reaction (iddPCR). The described method is not only sensitive but also allows multiplexing (currently up to three proteins). We used uniquely designed DNA barcoded antibodies for protein recognition. The labeled EV are encapsulated into 70 µm droplets in which PCR amplifies the message of the DNA barcode. Using different

Dr. J. Ko, Dr. J. C. T. Carlson, Dr. A. Marquard, J. Gungabeesoon,
Dr. M. J. Pittet, Dr. R. Weissleder
Center for Systems Biology
Massachusetts General Hospital
185 Cambridge St, CPZN 5206, Boston, MA 02114, USA
E-mail: rweissleder@mgh.harvard.edu
Dr. J. Ko, Y. Wang, Dr. D. Weitz
Wyss Institute for Biologically Inspired Engineering
Harvard University
Boston, MA 02115, USA

The ORCID identification number(s) for the author(s) of this article can be found under https://doi.org/10.1002/adbi.201900307.

Y. Wang, Dr. D. Weitz
John A. Paulson School of Engineering and Applied Sciences and
Department of Physics
Harvard University
Cambridge, MA 02138, USA
Y. Wang
Department of Chemistry and Chemical Biology
Harvard University
Cambridge, MA 02138, USA
Dr. J. C. T. Carlson, Dr. R. Weissleder
Harvard Cancer Center
Massachusetts General Hospital and Harvard Medical School
Boston, MA 02114, USA
Dr. A. Charest
Department of Medicine
Beth Israel Deaconess Medical Center
Boston, MA 02215, USA
Dr. R. Weissleder
Department of Systems Biology
Harvard Medical School
200 Longwood Ave, Boston, MA 02115, USA

**ADVANCED
SCIENCE NEWS**
www.advancedsciencenews.com

**ADVANCED
BIOSYSTEMS**
www.adv-biosys.com

barcode sequences and fluorophores, we show that it is possible to profile proteins in individual EV. We optimized the experimental conditions, validated measurements, and then applied EV profiling to PD-L1 measurements in cancer-cell derived EV.

2. Results

2.1. Description of the Single EV-iddPCR Technique

To reveal proteins of interest, we used target-specific monoclonal antibodies barcoded with unique and amplifiable DNA sequences. A number of routes to prepare such constructs have been described, including NHS/maleimide chemistry, photoaffinity labeling, and protein adaptors among others.[12–15] Here, we chose bioorthogonal *trans*-cyclocene/tetrazine (TCO/Tz) conjugation as it is cost effective and allows rapid, titratable, and readily purified labeling reactions. Barcoded antibodies were incubated with EV for labeling, followed by size exclusion chromatography (SEC) to remove unbound antibody–DNA (Ab–DNA) molecules (**Figure 1**A). The concentration of labeled EV in solution was then determined by nanoparticle tracking analysis (NTA), allowing us to adjust concentrations and flow rates to optimize the statistical likelihood of single EV encapsulation.[16–18] By encapsulating the Ab–DNA barcoded EV with a PCR master mix (BioRAD), the signal (if present) can be directly amplified in a given droplet (Figure 1B). Following PCR amplification, individual droplets were imaged by fluorescence microscopy to quantify the fraction of droplets containing EV with the target of interest (Figure 1C).

We used TCO/Tz chemistry to maximize labeling efficiency and minimize cost and time of Ab–DNA conjugation (**Figure 2**). Traditional bioconjugation reactions for ligating thio-DNA to malemide-modified antibodies require extended incubations with a significant molar excess of the DNA barcode. In pilot experiments, we noted that the separation of excess barcode from the labeled antibody caused considerable antibody loss. In contrast, the rapid reaction kinetics of TCO/Tz ligations allow the conjugation reaction to proceed to completion in just 30–60 min at matched stoichiometry, obviating the need to remove free DNA. We therefore labeled antibodies of interest (e.g., EGFR, EPCAM, PD-L1, CD4, CD8, GZMB, TCF7) with TCO-PEG$_4$-NHS (10 molar equivalents), purified the conjugates by gel filtration spin column, and achieved a degree of labeling (DOL) of 2–6 TCOs/Ab depending on the antibody and the initial protein concentration. In parallel, we functionalized amine-modified DNA barcodes with methyltetrazine-PEG$_4$-NHS, readily separating the excess Tz by gel filtration to isolate clean, exhaustively labeled Tz-DNA. The TCO-tagged antibodies were then conjugated with two equivalents of Tz-DNA; within 1 h, high yield Ab–DNA conjugates (DOL = 2) were obtained that did not require further purification. Figure 2 summarizes the three different barcode constructs synthesized. Each of the 65 bp barcodes contained a unique 20 bp recognition sequence flanked by a universal scaffold for PCR amplification. We designed forward and reverse primers to amplify the barcode and read-out probes with fluorochrome-quencher pairs in complementary channels for multiplexing: 6-carboxyfluorescein (6-FAM, ex/em 496/516) and HEX dye (ex/em 538/555) were paired with IowaBlackFQ; Cy5 (ex/em 648/668) was paired with IowaBlackRQ.

2.2. Droplet Microfluidics for Single EV Encapsulation

Following initial optimization procedures, we settled on the design of a simple two-channel droplet microfluidic device (**Figure 3**). This allowed us to separately introduce the EV and the PCR master mix. The latter contains all components necessary for the PCR assay such as DNA polymerase, dNTPs, MgCl$_2$, as well as enhancers and stabilizers in an optimized buffer. Due to the possibility of EV being lysed in the PCR master mix, labeled EV were added through a separate channel prior to droplet formation (Figure 3A). Using the
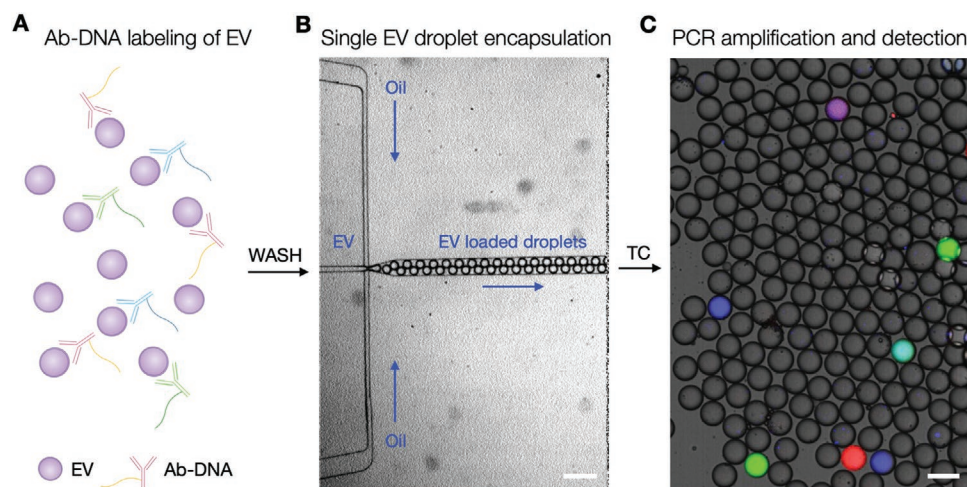

Figure 1. Schematic of droplet-based single EV detection. Single EV detection is achieved via three steps. A) First, EV are labeled with Ab–DNA conjugates for multiplexing and DNA-based detection of protein expressions. Remaining free Ab–DNA conjugates are then removed using size exclusion chromatography (SEC) before proceeding to the next step. B) Second, single EV are encapsulated in droplets by creating EV and PCR master mix containing water droplets in oil (scale bar = 300 μm). C) After thermal cycling (TC), EV that are labeled with targets of interest amplify and fluoresce for detection using imaging. (scale bar = 100 μm).
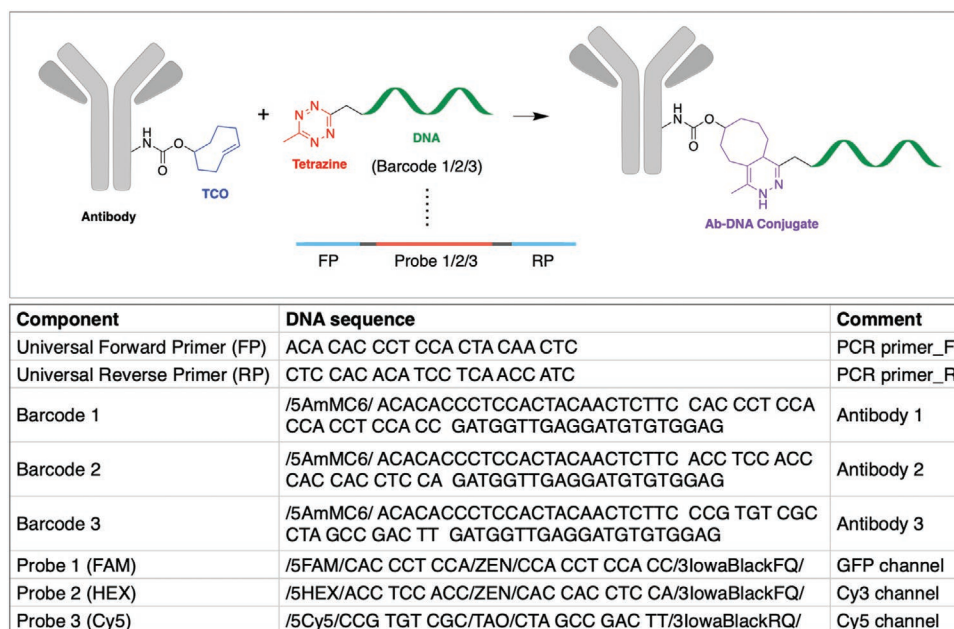
Component	DNA sequence	Comment
Universal Forward Primer (FP)	ACA CAC CCT CCA CTA CAA CTC	PCR primer_F
Universal Reverse Primer (RP)	CTC CAC ACA TCC TCA ACC ATC	PCR primer_R
Barcode 1	/5AmMC6/ ACACACCCTCCACTACAACTCTTC CAC CCT CCA CCA CCT CCA CC GATGGTTGAGGATGTGTGGAG	Antibody 1
Barcode 2	/5AmMC6/ ACACACCCTCCACTACAACTCTTC ACC TCC ACC CAC CAC CTC CA GATGGTTGAGGATGTGTGGAG	Antibody 2
Barcode 3	/5AmMC6/ ACACACCCTCCACTACAACTCTTC CCG TGT CGC CTA GCC GAC TT GATGGTTGAGGATGTGTGGAG	Antibody 3
Probe 1 (FAM)	/5FAM/CAC CCT CCA/ZEN/CCA CCT CCA CC/3IowaBlackFQ/	GFP channel
Probe 2 (HEX)	/5HEX/ACC TCC ACC/ZEN/CAC CAC CTC CA/3IowaBlackFQ/	Cy3 channel
Probe 3 (Cy5)	/5Cy5/CCG TGT CGC/TAO/CTA GCC GAC TT/3IowaBlackRQ/	Cy5 channel

Figure 2. Ab–DNA conjugation and DNA sequences. TCO-Tz click chemistry is used for Ab–DNA conjugation, enabling quantitative ligation of the Tz-functionalized barcodes to the TCO-tagged antibodies and eliminating the need for any washing steps. Sequences for universal primers for DNA amplification, DNA barcodes for barcoded antibody, and probes for fluorescence detection are included.

droplet microfluidic device, ≈70 µm droplets were created that contain both labeled EV and PCR master mix. To explore EV encapsulation conditions, we used 4 µm magnetic beads that could be easily visualized and thus served as a surrogate for small vesicles (Figure 3B). Following optimization, we settled on flow rates of 300 µL h⁻¹ master mix, 200 µL h⁻¹ EV solution, and 800 µl h⁻¹ oil that achieved a throughput of 727 droplets/sec. Taking into account the relevant dilution factor and droplet volume, the calculated EV input concentration would be expected to be 1.4×10^6 EV mL⁻¹ to achieve 0.1 EV per droplet. At this ratio, the Poisson distribution predicts that 9% of droplets will contain a single EV for readout, while 90.4%

of droplets will contain no EV (i.e., no signal), and just 0.45% will contain two EV.[16–18]

We next performed a series of measurements to validate the system, beginning with a determination of whether the number of EV could be measured accurately by iddPCR. EV from the Gli36-glioma cell line were universally labeled using NHS-PEG₄-TCO and Tz-DNA (Figure S1, Supporting Information). The labeled, NTA-measured EV were serially diluted and then counted by the iddPCR system. As shown in **Figure** 4A, there was linear agreement between two measurements ($R^2 = 0.99$). The limit of detection (LOD) of our system was 38 EV µL⁻¹ and the dynamic range was three orders of
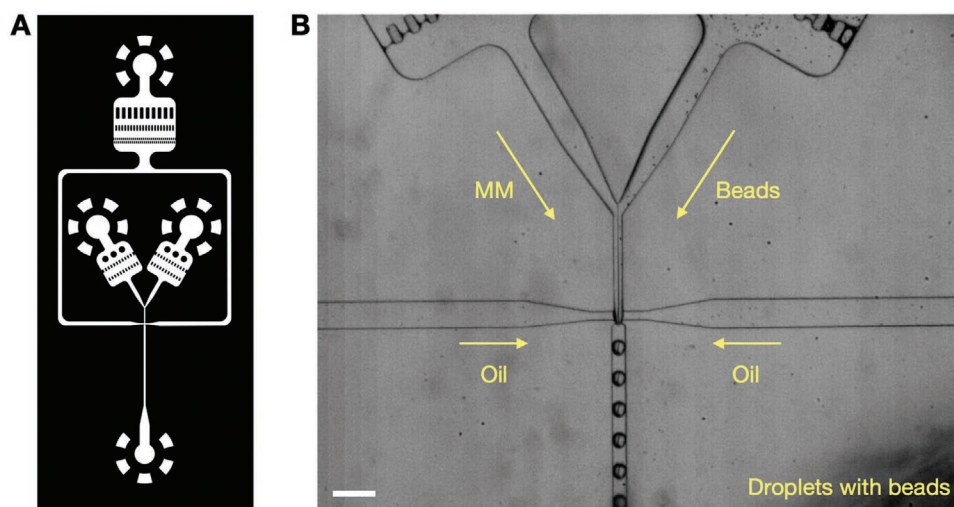

Figure 3. Droplet microfluidics design. A) Two-channel droplet microfluidic chips are designed for single EV analysis. PCR master mix and EV are introduced from each channel to form water droplets in oil. B) Microfluidic chip in operation with 4 µm beads for visualization (scale bar = 150 µm).

**ADVANCED
SCIENCE NEWS**
www.advancedsciencenews.com
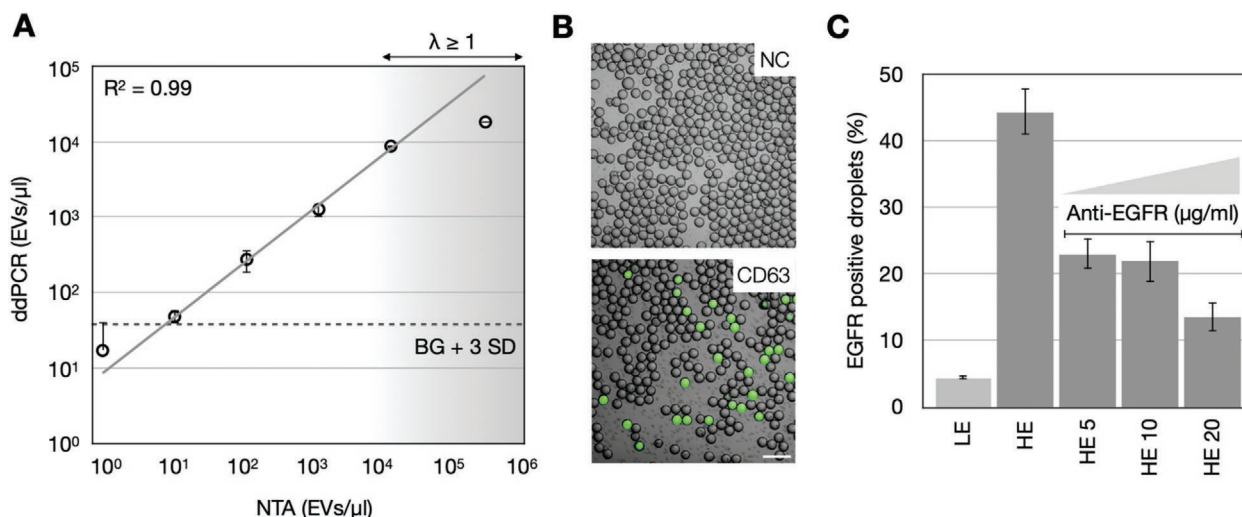
**ADVANCED
BIOSYSTEMS**
www.adv-biosys.com

Figure 4. Validation of ddPCR-based EV measurements. A) Titration curve. NTA-measured EV were serially diluted and counted by iddPCR. The limit of detection of our system was 38 EV μL^{-1} (BG: background, SD: standard deviation). For samples outside the digital range ($\lambda \geq 1$), the Poisson distribution was used to calculate the EV concentration from the observed fraction of negative droplets. The working dynamic range was three orders of magnitude, with a strong linear correlation between the NTA and ddPCR measurements ($R^2 = 0.99$). Error bars are standard deviations of $n = 3$ technical replicates. B) Representative microscopy examples of CD63+ positive droplets from iddPCR incubated with and without Gli36 EV (NC: negative control, Scale bar = 200 μm). C) Measurement of the fraction of EGFR positive EV obtained from U87 parental (LE = low expression of EGFR) and U87wt cells (HE = high expression of EGFR due to transfection). ($P < 0.0001$, one-way Anova). The EV were incubated with 10 μg mL^{-1} anti-EGFR–DNA conjugates. Note that the fraction of positive droplets decreases when inhibited with anti-EGFR (shown are 5, 10, 20 μg mL^{-1}) due to competitive inhibition. ($P < 0.001$, one-way Anova: each concentration to HE) (error bars are standard deviations of $n = 3$ technical replicates).

magnitude. EV concentrations that were over the digital analytical range ($\lambda \geq 1$) were calculated from the observed fraction of negative droplets and the expected Poisson distribution. Here, we measured the background of our platform using free Ab–DNA without EV and observed ≈14 positive droplets μL^{-1} of analyte (Figure S2A, Supporting Information). To measure the specificity of our platform, we labeled EV with nonspecific Ab–DNA (human IgG isotype control) and observed ≈44 positive droplets μL^{-1}. The purification efficiency of SEC was also measured by qPCR, comparing free Ab–DNA input to the post-column output, which indicated 99.97% removal of the free Ab–DNA (Figure S2B, Supporting Information).

We then labeled EV with a barcoded antibody against CD63, a reference marker with broad EV expression[29,30] and showed that we can identify CD63+ EV containing fluorescent droplets (Figure 4B) with low background levels concordant with our validation experiments. We next set out to assess our ability to detect EGFR in EV obtained from different cell lines known to vary in EGFR expression levels. We used two U87 cell lines that express either low levels of EGFR (U87 parental line) or high levels of EGFR (U87WT stably transfected with EGFR) as determined by flow cytometry, Western and immunohistochemistry.[19–21] EV were isolated from cell culture supernatant in parallel and quantified by NTA; iddPCR profiling of the matched samples showed that 44% of the high-EGFR expressing U87 EV were indeed positive for EGFR whereas a much smaller fraction was positive in the low-EGFR expressing cell lines (4%; Figure 4C). To corroborate iddPCR results, we performed competitive blocking experiments. Here, EV from high-EGFR expressing cells were preincubated with unconjugated anti-EGFR antibody (5–20 μg mL^{-1}) prior to Ab–DNA labeling (10 μg mL^{-1}). As expected, there was competitive inhibition as a function of blocker antibody concentration (Figure 4C).

2.3. Multiplexed Single EV Protein Analysis

We designed multiple antibody barcodes and probes to facilitate multi-protein analysis. In a first set of multiplexing experiments, we determined EGFR and EpCAM presence in EV obtained from Gli36 glioma cells. EV were isolated from cell culture supernatant using ultracentrifugation and incubated with a mixture of anti-EGFR-barcode1 and anti-EpCAM-barcode2. Following EV encapsulation into droplets, barcode 1 was read out with FAM-probe1 and barcode 2 was read out with HEX-probe2. Here, we used a higher EV loading density to facilitate assessment of signal/background characteristics of a double-positive droplet population. With 65% positive droplets overall, our results validate clean separation of barcode amplification in two spectral channels. A considerable fraction of droplets contained Gli36 EV that were positive for only EGFR (17%) or only EpCAM (9%) (**Figure 5**A). We also identified a double positive population (39%) predicted to contain a statistical admixture of droplets with single EV that carry both targets and multi-EV droplets in which both markers are detected.

While the iddPCR technique is very sensitive, it does not readily allow determination of protein expression levels (i.e., how much of EGFR or EPCAM resides in a given EV). Rather, since the technique is a digital one, it allows determination of the fraction of positive and negative EV for a given marker
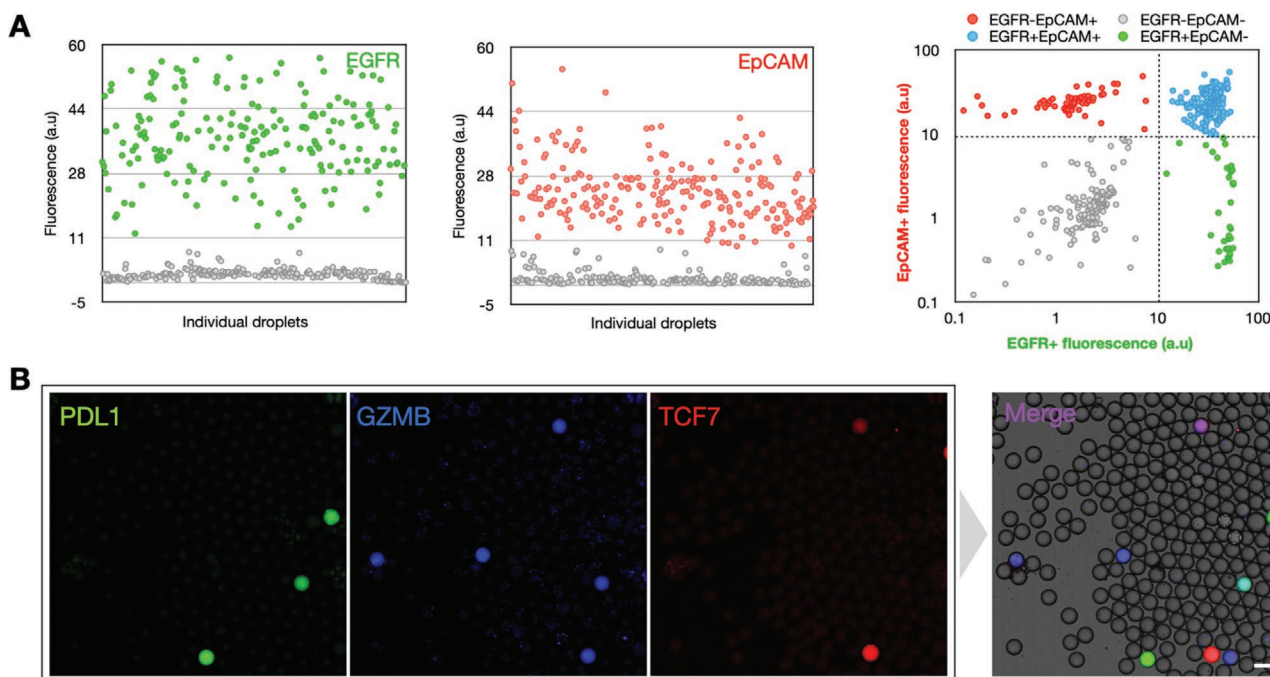
1900307 (4 of 8)

**ADVANCED
SCIENCE NEWS**

www.advancedsciencenews.com

**ADVANCED
BIOSYSTEMS**

www.adv-biosys.com

Figure 5. Multiplexed single EV protein profiling. A) Duplexing is developed and tested using EGFR and EpCAM protein profiling. Double positive (EGFR+ EpCAM+) EV subpopulation can be identified through multiplexing. Individual droplets are plotted (gray: empty or specific protein negative droplets, color: specific protein positive droplets). B) Single vesicle multiplexing was expanded to profile three targets (PD-L1, GZMB, and TCF7) from mouse plasma EV using FAM, HEX, and Cy5 fluorophores respectively (scale bar = 100 µm).

combination. To further expand the multiplexing to three simultaneous targets at low EV loading density, we chose a combination of immune markers: granzyme B (GZMB), transcription factor 7 (TCF7), and PD-L1 (Figure 5B).[22] These proof-of-principle experiments show that EV expressing these markers can be identified in mouse plasma of MC38 colon tumor-bearing mice and healthy mice ($n = 7$) (Figure 5B).[23] Multiplexing allows discovery of EV subpopulations that co-express multiple markers of interest, e.g. PDL1-GZMB positive (cyan) or GZMB-TCF7 positive (magenta).

EV are increasingly studied as biomarkers of disease and/or therapeutic efficacy.[24] Of particular interest in cancer is the tumor PD-L1 status, as it is a predictive biomarker of response to immunotherapy.[25] Moreover, PD-L1 present in cancer-cell derived EV can foster immune evasion.[26] We thus focused on profiling PD-L1 expression of single EV. The experiment assessed EV derived from different cancer cell lines (KP1.9, MC38, B16, Jurkat) and included CD4 and CD8 as positive/negative controls. **Figure 6**A shows bulk protein expression for the different markers in parental whole cells, as determined by flow cytometry. EV profiling measured positive fractions of EV subpopulations, which resulted in overall similar patterns: as expected, Jurkat cells and their EV were strongly positive for CD4; all three cell lines were negative for CD8 (control). At matched EV concentrations, MC38 EV had the highest PD-L1+ EV population (20.3%), followed by B16 EV (18.6%), and KP1.9 EV (8.6%; Figure 6B). These data are of scientific interest as they are the first to directly determine the quantity and fraction of PD-L1 positivity of single EV shed from parental tumor cells.

3. Discussion

The iddPCR technology developed here exploits an exponential PCR amplification step to ultrasensitively detect rare proteins of interest in single EV. While the markers examined to date have been on the EV surface, in principle the technique can be further extended to targets within the EV by semipermeabilization prior to Ab–DNA incubation. Overall, the method has unique advantages including i) very high detection sensitivity and signal-to-noise ratios (SNR); ii) facile multiplexing with distinct DNA barcodes; and iii) independence from the demanding microscopic resolution necessary to identify single EV.[5,6] Due to the digital characteristic of iddPCR, the system has the theoretical detection limit of a single copy of DNA, exponentially amplifying signals from very low EV protein to generate a brightly fluorescent 70 µm droplet. The typical amplified signal intensity in 70 µm droplets is robust and much easier to image compared to diffraction-limited 30–200 nm sized EV.

Like all measurement techniques, iddPCR also has certain limitations. While iddPCR is a high sensitivity technique due to its digital characteristic, it is not possible to obtain absolute expression levels of a given protein in EV due to possible PCR bias and extremely small amounts. To improve upon this, different linear amplification methods (e.g., in vitro transcription, IVT) or amplification tools that are less prone to bias (e.g., recombinase polymerase amplification (RPA), rolling circle amplification (RCA), combinations of linear and exponential amplifications) could be explored. A second limitation is the current level of multiplexing, which is limited to three colors. Multiplexing capabilities could be further improved by
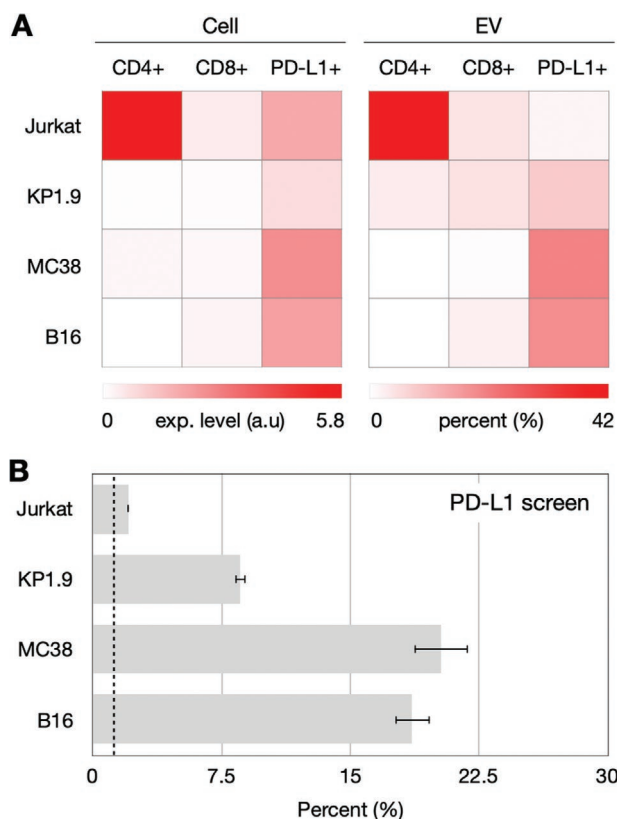
A

Figure 6. Cancer cell derived EV PD-L1 profiling. A) PD-L1 protein expression is measured with positive and negative control markers (CD4, CD8) from four different cancer cell derived EV (Jurkat, KP1.9, MC38, B16). The protein expression levels from cells are measured using flow cytometry and the positive fractions of EV subpopulations are measured using iddPCR. B) Percentage of PD-L1+ EV population is measured from cancer cell derived EV (error bars are standard deviations of $n = 3$ technical replicates) (P value < 0.0001 for Jurkat vs each cancer cell derived EV, one-way ANOVA).

allocating additional spectral channels to barcodes for imaging, or by using multiple barcode readouts via sequencing.

We developed the iddPCR EV method to ultimately detect rare proteins in single EV in clinical samples. The motivation for this is to eventually identify rare but highly predictive tumor cell derived EV ("tEV") defined by specific molecular markers. For example, the ability to detect mutant K-Ras protein in EV (KRASG12D, KRASG12V, others) would improve the diagnostic performance of EV cancer diagnostics. Similarly, one could detect other mutant cancer proteins (e.g., APC, TP53, PI3KCA, SMAD4, BRAF (V600E), BRCA1/2, EGFR (L858R, exon19 del, T790M), IDH1 (R132H), PTEN) if specific antibodies are or become available. Further, one could apply the multiplexing to detect multiple biomarker combinations (signatures) in tEV that are highly indicative of malignancy and in immune cell derived EV that are often defined by multiple markers (e.g., CD11b+ Ly6G Neutrophils). A number of such signatures have been described (e.g., QuadMarker).[27] We anticipate that the iddPCR approach will be a useful tool in the clinical assessment of patient-derived plasma EV and enable molecular signature detection and therapeutic monitoring.

4. Experimental Section

Device Fabrication: The microfluidic device for droplet generation was fabricated at the Soft Materials Cleanroom (SMCR), Harvard Center for Nanoscale Systems (CNS). The device ($h = 50$ µm) was made using soft lithography with SU-8 3050. The device dimensions are shown in Figure S3 (Supporting Information). The device was made hydrophobic before use by treating with 2% trichloro(1H,1H,2H,2H-perfluorooctyl)silane in Novec 7500 (Oakwood Chemical).

EV Isolation from Cells and Mice: U87 WT, U87 parental, B16, KP1.9, and MC38 cell lines were used to test and optimize the iddPCR technology. The U87 WT were described elsewhere.[21] U87 parental cells were received from the Charest lab (BIDMC) and the B16, KP1.9, and MC38 cells were received from the Pittet lab (MGH). Cells were grown in a 150 mm cell culture dish and expanded to 8–12 dishes for EV collection. Cells were grown and passaged in DMEM (10% FBS, 1% penicillin/streptomycin). Once confluent, media was changed to exosome-depleted DMEM (5% exosome-depleted FBS, 1% penicillin/streptomycin) and supernatant was collected 48 h after the media change. The collected supernatant was spun at 400 g for 5 min and filtered with a 0.22 µm vacuum filter (Corning) to remove any cellular debris. To obtain mouse plasma, size exclusion column (SEC) purification was used (Izon science, qEV Original column, 70 nm). After 3 mL of void volume, 1 mL of eluate was collected. Isolated EV size was measured using NTA; The Gli36 EV used in this study include 100–500 nm vesicles with an average size of 174.4 ± 57.3 nm (Mean ± SD) (Figure S4, Supporting Information). Experiments were approved by the MGH Institutional Animal Care and Use Committee (IACUC) and were performed in accordance with MGH IACUC regulations.

EV Isolation (Ultracentrifugation, Size Exclusion Column): For ultracentrifugation, cell culture supernatant was centrifuged (Beckman Coulter) at 100 000 g for 70 min at 4 °C for two times. The EV pellet was resuspended in PBS and aliquoted and stored in −80 °C until usage. For size exclusion chromatography, mouse plasma was loaded on the 70 nm qEV Original column (Izon science) and the protocol from the company was followed to collect EV from the sample.

EV Characterization (Qubit, NTA): After EV isolation, samples were characterized in two different ways. The protein concentration was measured using Qubit (Thermo Fisher) and the number of particles was calculated using NTA. For Qubit, the protein assay kit (Thermo Fisher) was used and the company protocol was followed for measurement. For NTA, the measurement was done at the Nanosight Nanoparticle Sizing and Quantification Facility at MGH using the NanoSight LM10. Three 30 s measurements were performed and averaged from each sample. The same parameters were used for analysis (Image: Screen gain of 7.4, Camera level of 11, Detection: Screen gain of 10, Detection threshold of 13).

EV Universal Labeling and Titration: To universally label Gli36 EV, EV solution was first buffer exchanged to PBS-bicarbonate buffer (100×10^{-3} M sodium bicarbonate in PBS, pH8.4) using a 40k Zeba column (Thermo Fisher, 87765). The EV was incubated with 250 molar equivalents of TCO-PEG$_4$-NHS Ester (Click Chemistry Tools, A137-10) for 1 h at RT after which unreacted TCO-PEG$_4$-NHS Ester was removed using a 40k Zeba column. TCO labeled EV was then incubated with 300×10^{-9} M Tz-DNA (see Experimental section: Ab–DNA conjugation) for 2 h at RT after which unreacted Tz-DNA was removed using the 70 nm qEV single column (Izon science). DNA labeled EV concentration was measured using NTA and titrated down by 10 fold for the iddPCR titration experiment.

Antibodies: Cetuximab (anti-EGFR antibody, Erbitux) and anti-CD63 antibody (Ancell, 215-820) were used to test and optimize the technology. Anti-CD4 (Bioxcell, BE0003-1, BE0288), CD8 (Bioxcell, BE0004-1, BE0004-2), and PD-L1 (Bioxcell, BE0285, BE0101) antibodies were used to profile immune markers from mouse samples. Anti-GZMB (PA5-13518, Thermo Fisher Scientific) and anti-TCF7 (MAB8224, R&D Systems) antibodies were to test for multiplexing. All antibodies were analyzed for the absence of BSA for Ab–DNA conjugation. All antibodies were tested on positive cell lines and validated before usage.

**ADVANCED
SCIENCE NEWS**

www.advancedsciencenews.com

**ADVANCED
BIOSYSTEMS**

www.adv-biosys.com

DNA Barcodes and Probes: DNA barcode and probe sequences used in this work are included in Figure 2. DNA barcodes were designed to have two universal regions for forward and reverse primers each and a unique sequence for dye-quencher probes that serve as a barcode for each marker of interest. For multiplexing, FAM, HEX, and Cy5 fluorophores were attached to the probes.

PCR Protocol: Three channel microfluidic device (EV, PCR master mix, oil) was used and ran at 200, 300, and 800 µL h^{-1} respectively (Harvard Apparatus). EV were diluted to achieve the desired target concentration per droplet based on the NTA results. ddPCR Supermix for Probes (BioRAD) was used as a PCR master mix and Droplet Generation Oil for Probes (BioRAD) was used. This combination showed the best droplet stability after thermal cycling at 95 °C. The concentration of probe was 125 × 10^{-9} M and that of primer was 250 × 10^{-9} M. The droplets were monitored using a high speed camera and collected in tubes for thermal cycling. The droplets were thermal cycled (Applied Biosystems) following the company protocol (BioRAD) for 35 cycles. Thermal cycled droplets were stored at room temperature for stability until imaging.

Ab–DNA Conjugation: BSA free antibodies were buffer exchanged to PBS–bicarbonate buffer (100 × 10^{-3} M sodium bicarbonate in PBS, pH8.4) using a 40k Zeba column (Thermo Fisher, 87 765). The antibody was incubated with 10 molar equivalents of TCO-PEG$_4$-NHS Ester (Click Chemistry Tools, A137-10) for 25 min at RT after which unreacted TCO-PEG$_4$-NHS Ester was removed using a 40k Zeba column. Degree of labeling (DOL) was checked by incubating antibodies with 10 molar equivalents of Cy3 Tetrazine (Click Chemistry Tools, 1018-1) for 25 min at RT before any remaining Cy3 Tetrazine was removed using a 40k Zeba column. Cy3:Antibody ratio was measured using the Nanodrop UV/Vis mode (Thermo Scientific) at A550/A280 and calculated from the known extinction coefficients of the dye (150 000 M^{-1} s^{-1}, CF280 0.05) and protein (215 000 M^{-1} s^{-1}).

1 × 10^{-3} M of amine-modified DNA oligo (Integrated DNA Technologies) was buffer exchanged to borate buffer (pH 8.5) using a 7k Zeba column (Thermo Fisher, 89 878). The DNA oligo was incubated with 20 molar equivalents of methyltetrazine-PEG$_4$-NHS Ester (Click Chemistry Tools, 1069-10) for 25 min at RT (10% DMF), after which excess Tz-PEG$_4$-NHS was removed by passage through three successive 7k Zeba columns. Tz:DNA ratio was calculated from Nanodrop UV–vis measurements at A520/A260 and the known extinction coefficients of the tetrazine (438 M^{-1}cm^{-1}) and DNA (as supplied by the manufacturer). Measurement at two different dilutions was required given the much stronger molar absorbance of the DNA.

TCO-labeled antibody and Tz-labeled DNA were mixed with appropriate DNA stoichiometry (Cy3:Antibody ratio minus 0.5, such that the TCO-antibody sites are in slight excess) and incubated for 45 min at RT. The conjugation was validated using the NuPAGE 4–12% Bis-Tris Protein Gel (Thermo Fisher, NP0321BOX). Unconjugated antibody and DNA-conjugated antibody were incubated with 4x NuPAGE LDS Sample Buffer (Thermo Fisher, NP0007) for 5 min at 75 °C and loaded to the gel with Novex Sharp Pre-stained Protein Standard (Thermo Fisher, LC5800). The gel was run in 20× NuPAGE MOPS SDS Running Buffer (Thermo Fisher, NP0001) for 1 h at 120 V. The validated antibody–DNA conjugate was stored in 4 °C until usage.

EV Labeling and Purification: EV were labeled with 10 µg mL^{-1} of Ab–DNA conjugates in 1% BSA–PBS for 1 h and purified by size exclusion chromatography (qEV single column, Izon science, 70 nm) to remove unlabeled Ab–DNA conjugates. Single use qEV columns were used to avoid cross-barcode contamination and 70 nm columns were used to include the 70–1000 nm EV range. After the EV solution was loaded, PBS was used to collect 1 mL of dead volume. The dead volume tube was discarded and 400 µL of eluate was collected in PBS to achieve a pure EV population. 2% loss after the qEV column-based purification was observed. Purification efficiency was checked using qPCR (Figure S2B, Supporting Information). The labeled EV were stored at 4 °C and used within a few days to prevent degradation.

Cell Flow Cytometry: Cells were collected fresh before staining. After PBS wash, cells were labeled with primary antibodies (5 µg mL^{-1}) for 30 min at RT, washed for two times, then labeled with secondary antibodies (2 µg mL^{-1};

Thermo Fisher) for 20 min at RT. The cells were washed for two times before flow cytometry. Propidium iodide (PI) was used to exclude dead cells for analysis. Flow data were analyzed using FlowJo.

Imaging and Image Analysis: Zeiss Axio Observer Z1 inverted fluorescence microscope (Wyss Institute) was used to acquire fluorescent images. GFP, Cy3, and Cy5 filter cubes were used to excite FAM, HEX, and Cy5 fluorophores, respectively. For imaging analysis, ImageJ and CellProfiler were used to measure fluorescent intensity and to count droplets.

Statistical Analysis: Normalization based on the background derived from each fluorescent channel for consistent analysis and comparison was performed. Outlier analysis was not performed to exclude any data. Error bars were included that represent standard deviations from $n = 3$ technical replicates. P values (One-Way ANOVA) were included to show statistically significant difference among and between experimental groups. Excel was used for statistical analysis.

Supporting Information

Supporting Information is available from the Wiley Online Library or from the author.

Conflict of Interest

The authors declare no conflict of interest.

Author Contributions

R.W., J.K., and M.P. designed this study. J.K., Y.W., J.G., and J.C.T.C. prepared the experiments. J.K. and all other co-authors analyzed and interpreted the data. R.W., J.K., and J.C.T.C. wrote the manuscript with the assistance of all other co-authors.

[1] R. Zilionis, C. Engblom, C. Pfirschke, V. Savova, D. Zemmour, H. D. Saatcioglu, I. Krishnan, G. Maroni, C. V. Meyerovitz, C. M. Kerwin, S. Choi, W. G. Richards, A. De Rienzo, D. G. Tenen, R. Bueno, E. Levantini, M. J. Pittet, A. M. Klein, *Immunity* **2019**, *50*, 1317.

[2] L. Yang, J. George, J. Wang, *Proteomics* **2019**, 1900226.

**ADVANCED
SCIENCE NEWS**

www.advancedsciencenews.com

**ADVANCED
BIOSYSTEMS**

www.adv-biosys.com

[3] E. Willms, C. Cabañas, I. Mäger, M. J. A. Wood, P. Vader, *Front. Immunol.* **2018**, *9*, 738.

[4] A. Gyuris, J. Navarrete-Perea, A. Jo, S. Cristea, S. Zhou, K. Fraser, Z. Wei, A. M. Krichevsky, R. Weissleder, H. Lee, S. P. Gygi, A. Charest, *Cell Rep.* **2019**, *27*, 3972.

[5] K. Lee, K. Fraser, B. Ghaddar, K. Yang, E. Kim, L. Balaj, E. A. Chiocca, X. O. Breakefield, H. Lee, R. Weissleder, *ACS Nano* **2018**, *12*, 494.

[6] K. Fraser, A. Jo, J. Giedt, C. Vinegoni, K. S. Yang, P. Peruzzi, E. A. Chiocca, X. O. Breakefield, H. Lee, R. Weissleder, *Neuro Oncol.* **2019**, *21*, 606.

[7] C. Campos-Silva, H. Suárez, R. Jara-Acevedo, E. Linares-Espinós, L. Martinez-Piñeiro, M. Yáñez-Mó, M. Valés-Gómez, *Sci. Rep.* **2019**, *9*, 2042.

[8] A. Morales-Kastresana, J. C. Jones, *Methods Mol. Biol.* **2017**, *1545*, 215.

[9] J. P. Nolan, E. Duggan, *Methods Mol. Biol.* **2018**, *1678*, 79.

[10] J. A. Welsh, J. A. Holloway, J. S. Wilkinson, N. A. Englyst, *Front. Cell Dev. Biol.* **2017**, *5*, 78.

[11] C. Liu, X. Xu, B. Li, B. Situ, Y. Pan, Y. Hu, T. An, S. Yao, L. Zheng, *Nano Lett.* **2018**, *18*, 4226.

[12] R. J. Giedt, D. Pathania, J. C. T. Carlson, P. J. McFarland, A. F. Del Castillo, D. Juric, R. Weissleder, *Nat. Commun.* **2018**, *9*, 4550.

[13] S. K. Saka, Y. Wang, J. Y. Kishi, A. Zhu, Y. Zeng, W. Xie, K. Kirli, C. Yapp, M. Cicconet, B. J. Beliveau, S. W. Lapan, S. Yin, M. Lin, E. S. Boyden, P. S. Kaeser, G. Pihan, G. M. Church, P. Yin, *Nat. Biotechnol.* **2019**, *37*, 1080.

[14] C. Stiller, H. Aghelpasand, T. Frick, K. Westerlund, A. Ahmadian, A. E. Karlström, *Bioconjugate Chem.* **2019**, *30*, 2790.

[15] G. A. O. Cremers, B. J. H. M. Rosier, R. Riera Brillas, L. Albertazzi, T. F. A. de Greef, *Bioconjugate Chem.* **2019**, *30*, 2384.

[16] D. J. Collins, A. Neild, A. deMello, A. Q. Liu, Y. Ai, *Lab Chip* **2015**, *15*, 3439.

[17] A. Huebner, M. Srisa-Art, D. Holt, C. Abell, F. Hollfelder, A. J. deMello, J. B. Edel, *Chem. Commun.* **2007**, 1218.

[18] S. Köster, F. E. Angilè, H. Duan, J. J. Agresti, A. Wintner, C. Schmitz, A. C. Rowat, C. A. Merten, D. Pisignano, A. D. Griffiths, D. A. Weitz, *Lab Chip* **2008**, *8*, 1110.

[19] M. M. Inda, R. Bonavia, A. Mukasa, Y. Narita, D. W. Sah, S. Vandenberg, C. Brennan, T. G. Johns, R. Bachoo, P. Hadwiger, P. Tan, R. A. Depinho, W. Cavenee, F. Furnari, *Genes Dev.* **2010**, *24*, 1731.

[20] M. Nagane, F. Coufal, H. Lin, O. Bögler, W. K. Cavenee, H. J. Huang, *Cancer Res.* **1996**, *56*, 5079.

[21] R. Nishikawa, X. D. Ji, R. C. Harmon, C. S. Lazar, G. N. Gill, W. K. Cavenee, H. J. Huang, *Proc. Natl. Acad. Sci. USA* **1994**, *91*, 7727.

[22] M. Sade-Feldman, K. Yizhak, S. L. Bjorgaard, J. P. Ray, C. G. de Boer, R. W. Jenkins, D. J. Lieb, J. H. Chen, D. T. Frederick, M. Barzily-Rokni, S. S. Freeman, A. Reuben, P. J. Hoover, A. C. Villani, E. Ivanova, A. Portell, P. H. Lizotte, A. R. Aref, J. P. Eliane, M. R. Hammond, H. Vitzthum, S. M. Blackmon, B. Li, V. Gopalakrishnan, S. M. Reddy, Z. A. Cooper, C. P. Paweletz, D. A. Barbie, A. Stemmer-Rachamimov, K. T. Flaherty, J. A. Wargo, G. M. Boland, R. J. Sullivan, G. Getz, N. Hacohen, *Cell* **2018**, *175*, 998.

[23] C. Engblom, C. Pfirschke, R. Zilionis, J. Da Silva Martins, S. A. Bos, G. Courties, S. Rickelt, N. Severe, N. Baryawno, J. Faget, V. Savova, D. Zemmour, J. Kline, M. Siwicki, C. Garris, F. Pucci, H. W. Liao, Y. J. Lin, A. Newton, O. K. Yaghi, Y. Iwamoto, B. Tricot, G. R. Wojtkiewicz, M. Nahrendorf, V. Cortez-Retamozo, E. Meylan, R. O. Hynes, M. Demay, A. Klein, M. A. Bredella, D. T. Scadden, R. Weissleder, M. J. Pittet, *Science* **2017**, *358*, aal5081.

[24] F. Pucci, C. Garris, C. P. Lai, A. Newton, C. Pfirschke, C. Engblom, D. Alvarez, M. Sprachman, C. Evavold, A. Magnuson, U. H. von Andrian, K. Glatz, X. O. Breakefield, T. R. Mempel, R. Weissleder, M. J. Pittet, *Science* **2016**, *352*, 242.

[25] S. P. Patel, R. Kurzrock, *Mol. Cancer Ther.* **2015**, *14*, 847.

[26] F. L. Ricklefs, Q. Alayo, H. Krenzlin, A. B. Mahmoud, M. C. Speranza, H. Nakashima, J. L. Hayes, K. Lee, L. Balaj, C. Passaro, A. K. Rooj, S. Krasemann, B. S. Carter, C. C. Chen, T. Steed, J. Treiber, S. Rodig, K. Yang, I. Nakano, H. Lee, R. Weissleder, X. O. Breakefield, J. Godlewski, M. Westphal, K. Lamszus, G. J. Freeman, A. Bronisz, S. E. Lawler, E. A. Chiocca, *Sci. Adv.* **2018**, *4*, aar2766.

[27] A. A. Ghazani, C. M. Castro, R. Gorbatov, H. Lee, R. Weissleder, *Neoplasia* **2012**, *14*, 388.

[28] Q. Tian, C. He, G. Liu, Y. Zhao, L. Hui, Y. Mu, R. Tang, Y. Luo, S. Zheng, B. Wang, *Anal. Chem.* **2018**, *90*, 6556.

[29] A. G. Cashikar, P. I. Hanson, *PLoS One* **2019**, *14*, e0220007.

[30] G. Corso, W. Heusermann, D. Trojer, A. Görgens, E. Steib, J. Voshol, A. Graff, C. Genoud, Y. Lee, J. Hean, J. Z. Nordin, O. P. B. Wiklander, S. El Andaloussi, N. Meisner-Kober, *J. Extracell. Vesicles* **2019**, *8*, 1663043.

1900307 (8 of 8)